Solid-State ^{13}C NMR Study of Thermotropic Polybibenzoates. 1. Poly(heptamethylene p,p'-bibenzoate) and Poly[oxybis(trimethylene) p,p'-bibenzoate]

Ernesto Pérez and Mónica M. Marugán

Instituto de Ciencia y Tecnología de Polímeros (CSIC), Juan de la Cierva 3, 28006 Madrid, Spain

David L. VanderHart*

Polymers Division, National Institute of Standards and Technology, Gaithersburg, Maryland 20899

Received May 7, 1993®

ABSTRACT: Solid-state ^{13}C NMR spectra of two chemically similar bibenzoate polymers, P7MB and PDTMB, were investigated at ambient temperature for different thermal histories. The spacer in P7MB includes a sequence of seven methylene groups; in PDTMB the central methylene group is replaced by an oxygen atom. These polymers both form smectic liquid crystalline (LC) phases as well as conventional crystalline (CR) phases. Signals from the CR regions were separated from those of the noncrystalline (NC) regions, and some information about inequivalences within the CR unit cells was obtained. A NMR comparison of quenched versus annealed PDTMB sought to contrast the LC behavior in the quenched sample versus the NC behavior in the annealed sample. Modest variations in relaxation times were observed, suggesting that the NC material in the annealed sample experiences modified constraints and, by implication, does not consist of a well-ordered LC phase. Synchrotron and certain DSC data also support the idea that crystallization disrupts the LC phase. For the LC phase, relaxation times observed are consistent with spacer motions (conformational interconversion) with strong spectral densities at megahertz frequencies; the mesogens, on the other hand, have dominant spectral densities of motion in the kilohertz range. It is also argued that the motions of the mesogens in this frequency range are large-amplitude and are not limited to 180° flips of the aromatic rings. By implication, there must be considerable dynamic disorder in the mesogenic layer in the LC phase. Based on several indirect arguments, it is speculated that formation of the polymeric smectic phase does not require significant topological disentanglement of chains; hence, for example, crystallization from the LC state does not produce high levels of crystallinity. Speculative interpretations are also offered in connection with the formation of a planar zigzag arrangement of the spacer methylene groups in CR P7MB and in connection with the stacking of mesogenic groups in both CR structures. Results are correlated with X-ray and DSC data.

Introduction

Mesophase structures found in liquid crystalline (LC) polymers have received considerable attention in recent years. They represent a state of order between long-range, three-dimensionally ordered crystals and the disordered amorphous or isotropic states. Thus, the LC phases are characterized by the absence of positional long-range order in at least one dimension[1] while a long-range orientational order is preserved. The latter is responsible for the anisotropic properties of these materials.

Several studies have been published related to the thermotropic LC character of polyesters derived from bibenzoic acid.[2-7] The smectic-type mesophases reported for these polybibenzoates possess relatively high isotropization enthalpies and entropies, indicating a considerable degree of order in the LC phase.

Some aspects of the thermotropic behavior of poly[oxybis(trimethylene) p,p'-bibenzoate], PDTMB, have been previously reported.[5] The properties of this polymer were also compared with those of poly(heptamethylene p,p'-bibenzoate), P7MB, the analogue polyester with an all-methylene spacer. The main influence of the central oxygen atom in the spacer of PDTMB is that crystallization is greatly inhibited, presumably because of the increase in flexibility introduced by the ether group. The result is that the mesophase of PDTMB can be easily quenched to room temperature with no appreciable sign of crystallinity appearing for several days. On the other hand, severe quenching conditions are necessary to prevent crystallization from the mesophase state in P7MB. For such quenched samples, subsequent annealing provides specimens with various levels of crystallinity. The persistence of the mesophase content of the NC regions during this crystallization is one of the questions we will address.

Solid-state ^{13}C NMR is a convenient tool for probing molecular organization in polymeric solids. Spectra observed in the presence of high-power proton decoupling and magic angle spinning (MAS)[8] usually possess good chemical shift resolution. It is typical that ^{13}C resonances arising from ordered crystalline (CR) regions will be distinguishable from those originating from disordered, noncrystalline (NC) regions; the former are generally characterized by (a) narrower lines[9] (reproducible local environment and conformation) and (b) chemical shifts which may be sensitive to CR conformation[10,11] and, by the same argument, distinct from the chemical shifts of corresponding carbons in the amorphous region.[12] Also, owing to the fact that motions in the CR regions are more restricted than in the amorphous regions, relaxation times such as the carbon longitudinal relaxation time, T_1^C, and the proton rotating frame relaxation time, $T_{1\rho}^H$, will generally be longer for nuclei in the crystal relative to the amorphous region.[13,14] The latter is especially true when T_g for the amorphous region lies above the temperature of measurement. Moreover, ^{13}C MAS spectra often reveal magnetic inequivalences in the CR unit cell for carbons that exhibit single resonances in solution;[8] this provides

® Abstract published in *Advance ACS Abstracts*, October 1, 1993.

0024-9297/93/2226-5852$04.00/0

Table I. ^{13}C Chemical Shifts[a] Corresponding to the Two Phases and Two Thermal Histories of PDTMB, Compared with Those in Solution

	CR phase		disordered phase		
carbon[b]	annealed	quenched	annealed	quenched	solution[c]
a	166.3		165.6	165.7	166.2
	165.4[d]				
	164.4[d]				
b	140.1		142[d]	142[d]	144.3
c,d	131.5		130.4	130.4	130.2 (=c)
					130.0 (=d)
e	125.3		126[d]	125[d]	127.2
1,3	69.9[d]		68[d]	68[d]	67.6 (=3)
	68.9		64[d]	64[d]	62.4 (=1)
	66.5[d]				
	64.7[d]				
	63.0				
2	29.6		30.0	29.8	29.4

[a] Uncertainty in chemical shift values is ±0.3 ppm unless otherwise indicated. [b] See Figure 1 for assignments. [c] In solution of deuterated chloroform.[18] [d] Imprecisely defined owing to partial resolution or broad resonances.

Table II. ^{13}C Chemical Shifts[a] Corresponding to the Two Phases and Two Thermal Histories of P7TMB, Compared with Those in Solution

	CR phase		disordered phase		
carbon[b]	annealed	quenched	annealed	quenched	solution[c]
a	166.3	165.2	165.4	165.3	166.3
	165.2[d]				
b	141.1	139.9	142[d]	142[d]	144.3
	140.0				
	139.2				
c,d	131.1	131.2	130.4	130.2	130.1 (=c)
					129.9 (=c)
e	125.0	125.0	126[d]	126[d]	127.2
1	66.5	66.5	66.1	66.2	65.1
2,3,4	33.2	33.1	29.4	29.4	28.9 (=2)
	30.6	30.6			28.6 (=4)
	29.1	29.1			25.9 (=3)
	28.3[d]				

[a] Uncertainties in chemical shift values is ±0.3 ppm unless otherwise indicated. [b] See Figure 1 for assignments. [c] In solution of deuterated chloroform.[18] [d] Imprecisely defined owing to partial resolution or broad line width.

valuable information for structure determination.[15,16]

The purpose of this work is to study samples of P7MB and PDTMB with different proportions of CR, NC, and LC phases in order to explore how solid-state ^{13}C NMR can be used to characterize these materials. Although one of our objectives was to isolate spectra of the pure LC phase, we were hindered in this pursuit because we could not produce pure amorphous samples nor could we be sure that other NC samples were fully LC. As will be seen, NMR observables provide an easy identification of the CR state but less contrast between the LC phase and amorphous states in these materials.

Experimental Section

The two polybibenzoates were synthesized by melt transesterification of the diethyl ester of *p,p'*-bibenzoic acid (4,4'-biphenyldicarboxylic acid) and the corresponding glycol, using isopropyl titanate as catalyst. Commercial heptamethylene glycol was used in the synthesis of P7MB, while 3,3'-oxydipropanol (the dimer of trimethylene glycol) was employed in the case of PDTMB. The details of the preparation and characterization of the dimer and the polyesters have been previously reported.[5,6,17] Moreover, the ^{13}C NMR spectra of the two polyesters in a solution of deuterated chloroform have been reported elsewhere.[18] The chemical shifts corresponding to the different carbons are presented in Tables I and II; assignments refer to the carbon designations shown in Figure 1. The PDTMB structure may be obtained by replacing carbon number 4 in this figure by an oxygen atom.

Polymer films of PDTMB and P7MB were quenched to room temperature from the isotropic state (200 °C). The quenching agents were air and liquid nitrogen, respectively. Half of each quenched sample was subsequently annealed: at 145 °C for 100 min for P7MB and at 70 °C for 24 days in the case of PDTMB. The quenched and annealed samples are designated by Q and A suffixes, respectively.

^{13}C spectra were taken at ambient temperature on a noncommercial spectrometer operating at 25.193 MHz (2.35 T). The probe incorporates a 7-mm rotor/stator combination made by Doty Scientific.[19] MAS frequencies were typically 3.5 kHz, and the nutation frequencies associated with the rf fields were 66 kHz for carbons and 69 kHz for protons. Cross polarization (CP) times were 1.5 ms for the spectra shown in the figures and 0.7 ms for relaxation measurements. These relaxation measurements included T_1^C, using the method of Torchia,[20] and $T_{1\rho}^C$ and T_2^C (carbon rotating frame and transverse relaxation times, respectively). The last two measurements are distinguished by variable periods inserted between the CP and observation windows of the usual CP experiment. For $T_{1\rho}^C$ there is spin locking of the carbon magnetization in the absence of proton decoupling. For T_2^C there

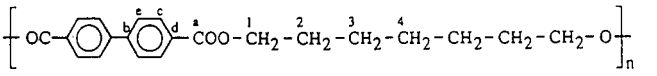

Figure 1. Chemical structure of P7MB with carbon designations. The structure of PDTMB is obtained by replacing the C_4 methylene group with an oxygen atom.

is a period, $2t_{echo}$, of proton decoupling spanning an even number of rotor periods; in the middle of this interval, a single 180° carbon pulse is inserted for refocusing chemical shift effects.

Ambient-temperature proton experiments were carried out on a Bruker CXP200 spectrometer operating at 4.7 T. A MAS probe, incorporating 5-mm rotors and made by Doty Scientific, was employed. Bloch decays were taken using a 60°, 1-μs excitation pulse with a 2-MHz filter width, a 4-μs dwell time, and a 2-μs dead time. T_{1xz} measurements[21] were conducted on a static sample (so as to avoid strong artifacts associated with the coupling of the chemical shift offset and the MAS-determined dipolar modulations) and utilized the MREV-8 multiple pulse sequence[22] with a 1.5-μs 90° pulse and a 38.4-μs cycle time. T_{1xz} rates for static samples are similar to $T_{1\rho}^H$ rates since similar frequencies of molecular motion contribute to each process.[21] An advantage of the T_{1xz} experiment is that the entire decay can be captured in a single acquisition.

X-ray diffractograms were obtained with an X-ray diffractometer from Philips Co. equipped with a Geiger counter detector, using nickel-filtered Cu Kα radiation.

Small-angle experiments were obtained at Daresbury Laboratory, U.K. (station 8.2), using synchrotron radiation. Rat-tail collagen (L = 67.0 nm) was used for calibration.

Results and Discussion

X-ray and Synchrotron. The X-ray diffractograms of the quenched and annealed samples of PDTMB and P7MB are presented in Figures 2 and 3, respectively. The quenched samples are rich in the LC phase which is most likely of the smectic-A type.[4,18] The only narrow features in the diffractogram of the quenched PDTMB sample correspond to the smectic mesophase,[5] while the broad peak exhibits a shape similar to that of the isotropic melt;[5] furthermore, 24 days of annealing at 70 °C are necessary to develop a rather small amount of three-dimensional order. By subtracting from the top diffractogram of Figure 2 a fraction corresponding to the diffractogram of the melt (not shown), a crystallinity of about 31% is deduced.

In contrast, for P7MB the transformation of the mesophase into a three-dimensional crystal is a fast process and even the sample quenched in liquid nitrogen exhibits a small amount of crystallinity. Moreover, relatively short annealing times are necessary to produce considerable

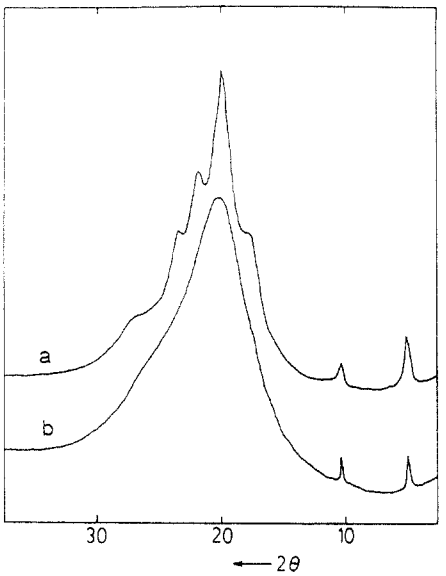

Figure 2. Ambient-temperature X-ray diffractograms of annealed (a) and quenched (b) PDTMB. For clarity, experimental noise, whose rms amplitude is less than 2% of the diffractogram maxima, has been removed by retracing.

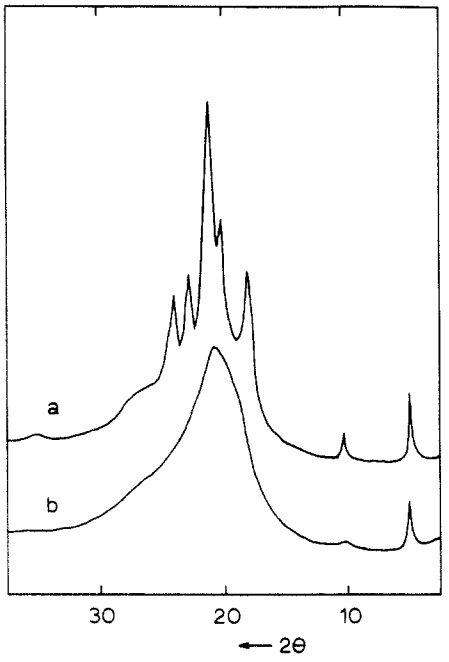

Figure 3. Ambient-temperature X-ray diffractograms of annealed (a) and quenched (b) P7MB. For clarity, experimental noise, whose rms amplitude is less than 2% of the diffractogram maxima, has been removed by retracing.

levels of crystallinity. In fact, from the diffractograms of Figure 3a,b, crystal contents of 47% and 17% are estimated for the annealed and quenched samples, respectively. The lack of sharp features in the diffractogram of the quenched sample indicates that smaller and/or imperfect crystals characterize this sample. Again, the diffractogram for the melt has been used as a reference for the NC material. While it is recognized that the melt is not necessarily an appropriate reference state for describing a phase which may well contain LC material, we justify its use by the following observation. For LC P7MB, obtained by cooling from the melt to 152 °C, except for the peaks at lower angles (which peaks arise from the smectic periodicity), the shape of the main peak at higher angles is very similar to the melt diffractogram.[6] A simplifying characteristic of the P7MB samples is that crystallinity does not increase upon storage at room temperature owing to a T_g of 41

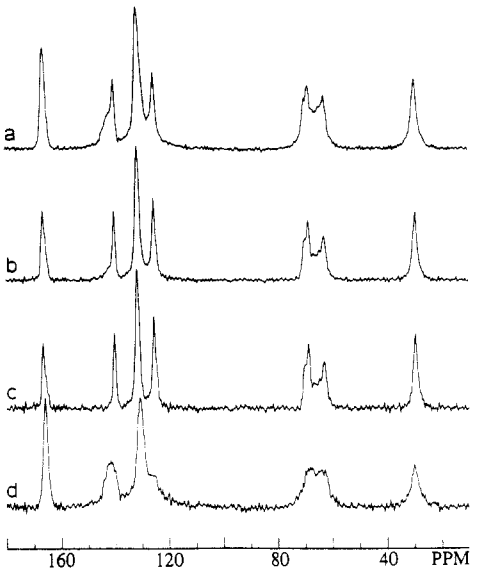

Figure 4. 25-MHz ^{13}C CPMAS spectra of annealed PDTMB at ambient temperature and the separation of these signals into spectra corresponding to the ordered and disordered regions. Spectra a and b are experimental spectra and correspond to proton spin lock (SL) times of 1 μs and 5 ms, respectively. Spectra c and d are linear combinations of spectra a and b where the criterion used for selecting a linear combination was the preservation or elimination of the broader wing of the C_b resonance near 142 ppm. Spectrum c represents the CR regions and d the disordered phase. Vertical scaling is arbitrary.

°C.[23] In both the annealed P7MB and annealed PDTMB diffractograms, a lower-angle peak is evident at a position very similar to that found for the quenched samples. The question arises whether, for the annealed samples, this represents a crystal repeat or indicates the coexistence of crystal and LC.

We have done recent measurements, using synchrotron radiation, to follow more precisely the position of the lower angle peak when going from the LC-rich quenched samples to the annealed semicrystalline samples. The instrumental resolution in the synchrotron experiments is superior to that in our X-ray experiments; therefore, the threshold for detection of small deviations is lower for synchrotron data. Preliminary ambient-temperature synchrotron data, taken using film samples, show periodicities corresponding to the first order peaks as follows: for PDTMB, 1.609 ± 0.004 and 1.622 ± 0.004 nm for freshly quenched and annealed specimens, respectively. Corresponding values for similar P7MB samples are 1.684 ± 0.005 and 1.662 ± 0.004 nm. Thus, there is a net shortening, by 0.022 ± 0.009 nm, of the repeat distance in P7MB in going from the quenched to the annealed sample and a lengthening of the repeat distance by 0.013 ± 0.008 nm in PDTMB. The shift of the position of this peak with crystallization, and in different directions, for the two homopolymers supports the notion that the repeat distances for the crystal lie very close to, but are distinct from, those of the LC state. Moreover, the shape of these peaks for the annealed samples shows that most of the intensity is shifted to the new location, implying that little, if any, of the periodicity associated with the former LC phase is preserved.

^{13}C Line Shapes. The ^{13}C CPMAS spectra of the annealed PDTMB sample acquired with variable proton spin locking (SL) times followed by a 1.5-ms cross polarization (CP) time are shown in Figure 4. Spectrum 4a is taken with a negligible SL time and is representative of the different phases present in the sample even though the relative proportions may be somewhat distorted owing to possible differences in CP efficiency. (The CP efficiency

Table III. Estimated $T_{1\rho}^{H}$ Values of the CR and LC Phases, and CR Fractions, f_c, Determined from Solid-State ^{13}C NMR and X-rays, for the Annealed, A, and Quenched, Q, Samples of the Two Polybibenzoates

	$T_{1\rho}^{H}$ (ms)		f_c	
sample	CR phase	disordered phase	NMR[a]	X-rays
PDTMB-A	14.8	2.6	0.28	0.31
PDTMB-Q		2.2	0	0
P7MB-A	12.6	3.8	0.39	0.47
P7MB-Q	7.7	3.2	0.14	0.17

[a] Corrected values (see text).

for each resonance in each region is dictated both by local $T_{1\rho}^{H}$ behavior and by the strength of dipolar couplings. Molecular motion determines both phenomena; therefore, especially when correlation times fall into the 10^{-5}–10^{-6}-s range, the CP efficiency is reduced since $T_{1\rho}^{H}$ relaxation achieves maximum rates and dipolar couplings begin to diminish.)

Spectrum 4a has both broad and narrow components; these are especially apparent in the aromatic resonance at about 140 ppm. Because of a shorter $T_{1\rho}^{H}$ associated with the NC material, the broad component loses relative importance as the SL time increases to 5 ms in 4b. On the assumption that there are only two components, CR and NC, in the spectrum, "pure-component spectra", generated via linear combinations of spectra 4a and 4b, can be associated with these two components. More than two components are not suggested by any line shape associated with single-carbon resonances. The criterion chosen for selecting a linear combination is the elimination of either the sharper or broader feature of the C_b resonance near 140 ppm. The spectra of the CR and NC components are shown, respectively, in Figure 4c,d. Moreover, the chemical shifts associated with the CR and NC component spectra are compiled in Table I; comparison is also made with chemical shift values from solution. The assignment of the spectrum with sharper features to the CR region is based on the idea that less mobile, regularly packed carbon sites have better defined chemical shifts than do more mobile (motionally broadened), more conformationally inhomogeneous carbon sites.[9] The apparent CR fraction, i.e. that fraction of spectrum 4c in 4a, is about 39%. However, a more appropriate estimate of the CR fraction is one which takes account of possible differences in $T_{1\rho}^{H}$ during the CP time of 1.5 ms. Using the relative intensity changes at the two SL times, one can estimate $T_{1\rho}^{H}$ for the two components and extrapolate to zero CP time. The corrected CR fraction is 28%. Such results are found in Table III. This corrected fraction is in reasonable agreement with the 31% deduced from the X-ray diffractograms.

Similar CPMAS experiments were performed on the quenched PDTMB sample. The corresponding spectra are presented in Figure 5. The most important feature of this figure is that the line shapes do not change with the SL time, indicating that $T_{1\rho}^{H}$ is quite uniform throughout the sample. A simple interpretation is that there is only a single phase present, which, judging by the WAXS results, is the LC phase. Yet, it is possible that the quenched sample is not entirely LC, but rather a mixture of LC and amorphous regions, each region possessing similar $T_{1\rho}^{H}$ relaxation behavior. We expected (but did not see) some contrast in line shapes or $T_{1\rho}^{H}$ behavior associated with the LC and amorphous phases. Our expectations were based on the structural constraints implied by the substantial enthalpies and entropies of isotropization associated with the mesophases of these

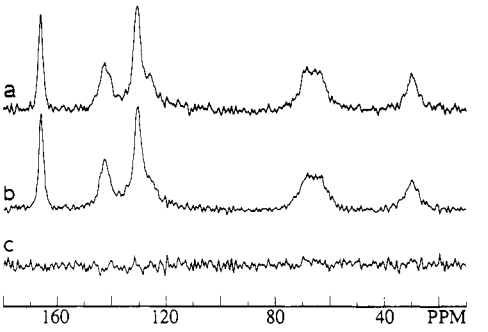

Figure 5. ^{13}C CPMAS spectra of quenched PDTMB: (a) SL time = 2 ms, (b) SL time = 1 μs, and (c) = (a) − (b). Vertical scaling is chosen for line shape comparison.

polybibenzoates[5,6] and by the restricted conformational freedom required to generate the periodicity of the LC phase.[4,7]

Even though Figure 5 shows a single line shape implying a single phase, it is possible that in using a 1.5-ms CP time, one could miss the signal associated with a second (amorphous) phase. Usually, there are three ways to miss or not distinguish a signal: first, molecular motion could be isotropic and fast such that no average dipolar coupling would exist and CP intensities would be largely quenched. This we found was not the case since the Bloch decay proton spectrum had less than 1% of its intensity associated with a sharp resonance. Second, it is possible that molecular motion would have correlation times in the 10^{-5}–10^{-7}-s range where $T_{1\rho}^{H}$ could become shorter than 1.5 ms and proton-decoupled ^{13}C line shapes would broaden considerably. To test for the fast $T_{1\rho}^{H}$ component, we measured the related T_{1xz} profile for protons using a nonspinning sample. There was a decay of about 50% over 1 ms, but no component had a shorter time constant. Therefore, we repeated the CP experiment using a CP time of 0.3 ms. While the relative intensities of the various lines in the spectrum differed slightly from those at 1.5-ms CP time, as expected, the shapes of corresponding resonances remained the same. Third, the minimum dimensions of the amorphous or LC domains could be small relative to the distance (≈4 nm) over which spin diffusion could equilibrate polarization in a time scale of $T_{1\rho}^{H}$ (2.2 ms). We discount this possibility under the assumption that, in order to generate the relatively narrow synchrotron peak, the minimum dimension of the LC phase should greatly exceed 4 nm (about two interplanar spacings). Thus, no candidate line shapes emerged which could differentiate the amorphous from the LC line shape. We conclude that if both amorphous and LC regions coexist, their spectra and/or their $T_{1\rho}^{H}$ relaxation characteristics are very similar. As a qualitative comment, the magnitude of the isotropization enthalpy, 19 J g^{-1}, for the LC phase of quenched PDTMB,[5] is comparable to the enthalpies of molecular smectic LC materials with molecular size and structure similar to the PDTMB monomer.[24] Since the latter materials are fully LC, this suggests that a substantial portion, if not the entire quenched PDTMB sample, is LC.

The spectrum corresponding to the CR phase in the annealed PDTMB sample (Figure 4c) exhibits upfield shoulders in the carbonyl resonance near 166 ppm, indicating the presence of inequivalent carbons in the unit cell of this polymer or multiple CR structures. Moreover, the relative intensities and the number of signals associated with carbons 1 and 3 (see Figure 1, Table I) are also incompatible with one crystal habit and a single monomer per unit cell. We note that if standard bond angles for the

Figure 6. ^{13}C CPMAS spectra of annealed P7MB: (a) SL time = 1 μs, (b) SL time = 8 ms, (c) SL time = 13 ms, (d) linear combination spectrum (representing the CR regions) generated from (b) and (c), and (e) linear combination spectrum (corresponding to the disordered regions) generated from spectra a and b. Note the multiplicity of CR sites implied by the C_b resonance in (d).

Figure 7. ^{13}C CPMAS spectra of quenched P7MB: (a) SL time = 1 μs, (b) SL time = 5 ms, (c) and (d) are linear combination spectra generated from (a) and (b) and represent the disordered and CR regions, respectively.

spacer are assumed, the parallel orientation of successive mesogenic units, separated by an odd number of backbone atoms in the spacer, is only permitted when the spacer forms a fold. When successive mesogens are found in adjacent mesogen layers, parallel orientation is forbidden.[18] Hence, unless every monomer in the crystal contains a fold, the unit cell will probably have a length incorporating at least two consecutive monomers. Magnetic inequivalence must be allowed for when solving the (as yet undetermined) crystal structure of PDTMB.

For P7MB, the corresponding CPMAS spectra, taken with different spin locking times, plus the broad and narrow pure components (obtained by linear combinations of the experimental spectra) are shown in Figures 6 and 7, for the annealed and quenched samples, respectively. The chemical shifts are given in Table II, along with those found in solution. Carbons c and d, with very similar chemical shifts in solution, cannot be resolved in the solid-state spectra (the same applies for PDTMB). The spectral region corresponding to carbon numbers 2–4 is composed of at least four resonances in the pure CR spectrum, Figure 6d, of the annealed sample. The solid-state assignment for these carbons is ambiguous since the chemical shifts are very close to one another and they may be in a different order than in solution. We note that the chemical shift of the most downfield resonance in this cluster is nearly identical to the chemical shift (33.11 ppm at 25 MHz) of the all-trans chains in linear (orthorhombic) polyethylene.[25] The intensity of this line is also approximately 20% of the total intensity in this region and would thus correspond to a single carbon. We speculate that this 33.2 ppm peak belongs to C4 and its shift may imply that it is in an all-trans conformation with no γ-gauche[26] effects. The implication is that all seven methylene carbons would be in a planar zigzag arrangement and any departures from the extended chain conformation in the crystal would have to involve the ester linkage.

It can be observed that the pure broad components (spectra 6e and 7c) look very similar for the two samples, with the expected feature of a much higher proportion of this component in the quenched sample. Furthermore, the spectra corresponding to the narrower components (Figures 6d and 7d) seem to be slightly different, as the resonances at about 140 and 165 ppm appear to be singlets in the quenched sample while they show multiplicity in the annealed specimen. The good correspondence of most other resonance positions would lead us to conclude that a slightly poorer resolution for CR resonances in the spectra of the quenched versus the annealed samples was the most probable explanation, rather than a different crystal form. It is our experience in dealing with materials like polyethylene and cellulose that resolution deteriorates when the crystallite size gets smaller or when crystal defects become more numerous. It is likely that such effects account for the different levels of resolution between spectra 6d and 7d. This interpretation is also consistent with the lack of sharp features at the higher angles in Figure 3b. Aside from a loss of resolution, there are no regions of major intensity contrast in Figures 6d and 7d; this observation provides some support for the claim that only one unit cell is present. If spectrum 6d corresponds to one crystal form, other implications follow. The resonance of carbon b near 140 ppm arises from two carbon sites per monomer, but the intensity profile shows at least three chemical shifts. The minimum number of monomers per unit cell would be 2 and even then there would be magnetically inequivalent benzene rings in at least one of the monomers; i.e. unit cell symmetry would be quite low. Incidentally, we dismiss the idea that some of the sharp features associated with the resonance of carbon b could arise from the LC phase since the LC phase in the quenched sample does not show these sharp features even though the LC phase is more abundant in this sample.

The apparent crystallinity, i.e. the proportion of spectrum 6d in 6a, is about 46% for the annealed sample while the proportion of spectrum 7d in 7a is about 18% for the quenched material. These apparent fractions can be corrected with the $T_{1\rho}^{H}$ values (crudely estimated from the spectra with different SL times) given in Table III. The corresponding crystallinities are 39 and 14% for the annealed and quenched samples, respectively, which

compare very well with the values estimated from the X-ray diffractograms.

For both PDTMB and P7MB, the C_b resonance at 140–144 ppm shows considerable sensitivity to its environment. In particular, the resonances in the CR regions are diamagnetically shifted about 2 ppm with respect to the broader NC or LC resonances and about 4 ppm with respect to the liquid-state shifts. If we understood the origin of these shifts better, we might be able to comment more definitively on the LC and CR states. We are tempted, in interpreting the diamagnetic shift of the CR resonance, to consider ring current shifts as the principal effect, even though we cannot insist on this since other effects such as mesogen-ring coplanarity or other effects of packing may well contribute. Nevertheless, since ring current shifts may be easily calculated,[27] we pursue this exercise. In order to generate strong diamagnetic shifts, one must position the C_b atoms, more or less, near the line formed by the hexad axis of a nearby ring. For the C_b carbon, a packing favorable for producing a diamagnetic shift occurs when the ring planes of neighboring mesogens are parallel (ring spacing assumed to be 0.4 nm) and when mesogen directors are inclined at about 60° with respect to the assumed plane containing all neighboring mesogens. This geometry produces near maximum ring current shifts from the two nearest-neighbor mesogens; moreover, it is a geometry which seems consistent with the condition found,[18] when using idealized bond geometries, that the angle between 1,4 aromatic axes for rings in adjacent mesogens on the same chain is about 60°. The magnitude of the resulting diamagnetic shift from the two nearest rings is about 1.7 ppm. If ring current effects are also the major reason for the chemical shift dispersion seen in the LC and NC phases, then considerable disorder between adjacent mesogens in the LC phase is implied.

Relaxation Times. We have conducted T_1^C, $T_{1\rho}^C$, and T_2^C experiments on both the PDTMB-Q (Q) and PDTMB-A (A) samples in order to arrive at some qualitative conclusions about the LC phase which, we believe, dominates the Q sample. We also use these data to comment on whether there is a significant difference between the Q sample and the NC-A material, i.e. the NC regions of the A sample. Rather than report all of the data, we will simply select the data critical to each argument; data omitted do not conflict with the conclusions made.

First, there is support in the relaxation data for the idea that the Q sample looks like a single phase; i.e. if both LC and NC phases coexist, then they behave similarly. The principal support is that the T_1^C recovery of the O–CH_2 and the CH_2 carbons is exponential with respective T_1^C's of 0.15 and 0.13 s. These are the fastest relaxing carbons, and their T_1^C's are comparable[12] to those of NC polyethylene where there is substantial conformational interconversion at ambient temperature at greater than megahertz rates. The next fastest relaxing carbons ($T_1^C \approx 1.5$ s) are the protonated aromatic carbons (PAC) resonating at 125 ppm. These are the C_e carbons in Figure 1. The T_1^C decay of these carbons is exponential within experimental error. T_1^C decays for the nonprotonated carbons are nonexponential. These decays cannot be used as criteria for the existence of multiple phases owing to the likelihood of ^{13}C–^{13}C spin exchange[28] with protonated carbons. The T_2^C and $T_{1\rho}^C$ decays of the protonated carbons were also quite exponential. However, in the presence of anisotropic motion these decay curves can, in principle, display more orientation-dependent dispersion than T_1^C does (in the absence of spin exchange).

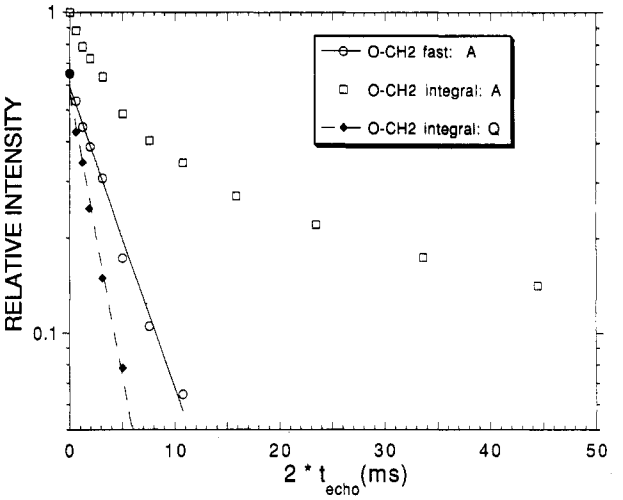

Figure 8. T_2^C decay profiles for O–CH_2 carbons in quenched and annealed PDTMB. Curves are defined in the legend. The faster decay in the annealed sample is associated with the NC regions and has been extracted from the overall decay using a two-exponential analysis. The decay for the quenched sample is arbitrarily scaled for comparison with this NC decay. The lines through the data represent exponential fits to each curve. The difference in the decay rates of these two faster-decaying curves implies that the LC- and the NC-annealed regions differ in some modest way.

The second point we make in reference to the PDTMB relaxation data is that we see some differences in relaxation between the Q (LC) state and the NC-A state; thereby supporting the thesis that the NC regions of the semicrystalline material differ from the LC state. We illustrate this in Figure 8 where T_2^C decays are shown for the O–CH_2 carbons in the Q and A samples. The A decay has a fast and slow component with time constants (using a two-component exponential model) of 4.3 ms (65%) and 48 ms (35%). The 4.3-ms faster decay (whose amplitude is consistent with the complementary apparent crystallinity in the CP spectrum) is about half as fast as the 2.3-ms T_2^C observed in the Q sample. The implied homogeneous broadening of the aliphatic lines in the Q and NC-A spectra is respectively 5.5 and 3.0 ppm. This difference can be seen in the O–CH_2 (and more easily in the parallel-behaving CH_2) lines in spectra 4d and 5b; the aliphatic lines in 5b are broader. In addition to this 4.3 versus 2.3 ms T_2^C contrast, the following changes in relaxation, Q to NC-A, are also observed: for T_1^C, 0.13 to 0.17 s (CH_2), 0.15 to 0.21 s (O–CH_2); for $T_{1\rho}^C$, 2.5 to 4.5 ms (aliphatic carbons), 0.8 to 1.5 ms (PAC at 120–125 ppm); and for T_2^C, 4.7 to 8.0 ms for the broader C_b resonance at 140–144 ppm. Note that changes in relaxation for the aromatic carbons just mentioned do not depend on deconvoluting relaxation curves for the A sample; these NC-A features are directly observed owing to chemical shifts between the CR and NC signals. The foregoing changes in relaxation times, while not dramatic, point to modest changes in system constraints on motion in the NC-A regions relative to the Q (LC) sample.

Two other qualitative insights relating to motions in the Q (LC) phase were obtained. First, the PAC at 120–125 ppm had the shortest $T_{1\rho}^C$ (0.8 ms); aliphatic carbons were next shortest (2.5 ms). Thus, if we make the simple assumption that motions of a single correlation time contribute to each of the measured relaxation times, including those cited below, observed for either the aliphatic or mesogenic carbons, one would estimate the correlation times for aliphatic motion to be about 10^{-7} s and for mesogenic motion to be about 10^{-4} s. Thus, motion is much more sluggish in the mesogenic layer than in the

spacer layer, as is expected. Second, with respect to the aromatic motions, we can make a good case that these motions are *more extensive* than simple 180° flips about the 1,4 axes of the rings. If so, the LC mesogen packing must allow for considerable dynamic disorder. The argument for motions, more than 180° flips, in the Q (LC) state is as follows: The PAC at 120–125 ppm has a $T_{1\rho}^C$ and a T_2^C of 0.8 ms while the C_b carbon, which is unprotonated and lies on the 1,4 axis, has a $T_{1\rho}^C$ of 16.5 ms and a T_2^C of 4.7 ms. According to Garroway et al.,[29] $T_{1\rho}^C = T_2^C$ for nonspinning samples where only motional modulation of the C–H dipolar interaction determines $T_{1\rho}^C$ and T_2^C, assuming equal nutation frequencies for the carbon and proton rf fields (66 and 69 kHz in our case). For all of the protonated carbons in PDTMB-Q, this equality holds, even in the presence of spinning. However, for the C_b resonance, T_2^C is 4.7 ms and $T_{1\rho}^C$ is 16.5 ms. This latter inequality implies that this T_2^C is not dominated by the C–H dipolar mechanism. That is a sensible conclusion also from the perspective that the T_2^C of the C_b carbon is short considering the 0.8-ms T_2^C of the adjacent PAC. The dipolar contribution to the T_2^C of C_b can be estimated from that of the adjacent PAC. The C_b carbon is about 0.214 nm from each of the two protons; hence, considering only the r^{-6} dependence of the dipolar contribution to both $T_{1\rho}^C$ and T_2^C, one would predict about a 30-fold increase in these quantities over the 0.8-ms values found for the PAC. Moreover, a consideration of the angular terms implies a greater than 30-fold increase in the event that motions were confined to 180° ring flips. Considering the observed 6-fold (4.7/0.8) ratio in the T_2^C's of C_b and the PAC, the T_2^C of C_b must be dominated by a nondipolar mechanism and this mechanism must further provide a weaker contribution to $T_{1\rho}^C$ than to T_2^C. The most probable mechanism, especially for an aromatic carbon is motional modulation of the chemical shift tensor.[9,30] During MAS, modulations which occur at ν_r and $2\nu_r$ can cause dephasing in the T_2^C experiment. By comparison, coupling of this mechanism to $T_{1\rho}^C$ is weaker when frequencies of motion are less than 66 kHz, the frequency which influences our $T_{1\rho}^C$ measurement. Since C_b lies on the 1,4 axis, 180° flips about this axis will not cause any modulation. Hence, in order to explain this 4.7-ms T_2^C, aromatic ring motions occuring at frequencies in the low kilohertz regime and with geometries substantially departing from 180° flips must be present. Thus, the mesogens in the LC phase at ambient temperature in PDTMB-Q must be characterized by a substantial dynamic disorder.

We looked to the full width at half-height of the synchrotron peak for PDTMB-Q as a possible measure of the disorder in layer spacing which could be tolerated in the LC; this measure gave 1.609 ± 0.025 nm. However, the width of the synchrotron peak is determined both by the reproducibility of each layer spacing and by the number of layers.[31] Hence, if the number of layers is large and the time average of each spacing is very uniform, it is likely that instantaneous fluctuations in layer spacings are considerably larger than the ±0.025 nm obtained from the line width.

Given that the synchrotron results for quenched and annealed PDTMB and P7MB are consistent with a disruption or modification of the LC phase upon crystallization in the annealed samples, and given that the ^{13}C relaxation data for PDTMB also support the inequivalence of the Q (LC) and the NC-A regions, we mention the following DSC result. P7MB presents a monotropic behavior on melting;[6] i.e. the crystal is transformed directly into the isotropic state. Moreover, it was shown[6] that in samples having different levels of crystallinity, two distinct endotherms appear at about 160 and 167 °C corresponding, respectively, to the isotropization of the untransformed mesophase and then to the melting of the crystals. The level of crystallinity influences the magnitude of each peak but has little effect on peak positions. Since a thoroughly crystallized sample exhibits a DSC endotherm corresponding only to the melting of the crystal and since the X-ray diffractogram and the NMR spectra of the same sample indicate no more than a 50% crystallinity, then it follows that, upon annealing, most of the LC phase has either disappeared or has been modified so that its endotherm coincides with that of the crystalline state. We favor the disappearance idea because of the just-mentioned stability of the peak positions; however, this is not an absolute proof. In any case, this is further evidence that crystallization, which takes place in the presence of the mesophase, proceeds by disrupting, or at least modifying, LC order. Corresponding DSC-based arguments for PDTMB are ambiguous since PDTMB exhibits regular thermotropic behavior[18] on heating; i.e. the endotherm corresponding to the transition from the crystal to the mesophase is obtained first, at 101 °C, while the isotropization of the mesophase appears subsequently at 172 °C. Therefore, thermal evidence for the presence of the mesophase is never seen while the crystalline state is present.

If the LC phase is disrupted or altered by crystal growth, then it also follows that the lower-angle scattering peak, which is found at very similar positions for either pair of quenched and annealed samples, points to nearly identical periodicities associated with the LC and CR phases, assuming that this peak arises mainly from crystal periodicity in the annealed samples. It is not obvious why these periodicities are similar or if this result is general.

Conclusions

Considerable information about inequivalent sites within the CR unit cells of these thermotropic polybibenzoates is obtained from solid-state ^{13}C NMR measurements. Also two speculative comments about the CR materials were offered, namely, that the mesogen planes consist of tilted, coplanar neighbors and that the methylene carbons in P7MB form a planar zigzag array.

The ^{13}C line widths and relaxation times of the LC phase of these polymers are quite typical of the disordered phases of nonmesogenic polymers; thus, there must be considerable dynamic and positional disorder tolerated within the smectic LC phase. At ambient temperature the role of the mesogen in stabilizing the LC phase is reflected in its lower frequency of motion (low to midkilohertz range) relative to the motional frequency of the spacer (megahertz range). In addition, evidence for dynamic disorder within the mesogens is also present. In this context, the close similarity of the main peak in the X-ray diffractograms at 152 °C (LC-containing phase) and 182 °C (isotropic melt) reinforces the idea that the smectic phase possesses considerable disorder.

There may be an initial expectation that, just as for the polymeric nematic state, the formation of a polymeric smectic LC phase should be accompanied by some corresponding topological requirements, such as chain disentanglement. Related to this, we offer the following comments. From the heats of isotropization in quenched PDTMB and from our inability to distinguish the presence of more than one phase, we conclude that the LC phase (as opposed to an amorphous phase) strongly dominates

this sample. Yet, prolonged annealing from this LC phase produces a crystallinity of only about 30%. Given that the smectic layer spacing is considerably shorter than the extended chain, many different conformations of the spacer can satisfy the layer spacing (in fact, loops are also permitted). Thus, some chain entanglements might be tolerated within the LC. This leads us to speculate that the polymeric smectic phase does *not* represent a topologically disentangled state, and this may be an important consideration from a polymer processing point of view. Indeed, certain authors have invoked chain folding of polymers in LC nematic[32] and smectic[33] states and this folding could be the origin of some entanglements. Also, in this picture of the entangled smectic phase, the process of crystallization injects topological constraints into NC regions with the result that a higher density of disorder must be accepted in these formerly LC regions. We have presented arguments from synchrotron, DSC, and ^{13}C relaxation data which support the thesis that crystallization significantly modifies the LC phase. Yet, on the basis of the contrast in NMR relaxation times between the LC and the NC regions of the semicrystalline samples, this modification of the LC phase produces only modest changes in molecular motion. Hence, it would be surprising to us if such NC regions were typified by a thorough intermingling of spacers and mesogens. Rather, in view of the thermodynamics which originally dictated the LC phase, we would still expect a significant spatial alternation of spacers and mesogens in the NC regions.

Acknowledgment. The financial support of the Comisión Interministerial de Ciencia y Tecnología (Project No. MAT91-0380) and of the Consejería de Educación de la Comunidad de Madrid is gratefully thanked. Also we acknowledge the support of NATO (Grant CRG 920094) in facilitating this interlaboratory collaboration. Dr. W. Bras and the Daresbury Laboratory (U.K.) are also thanked for their assistance in the synchrotron experiments. Helpful conversations with Drs. E. A. DiMarzio and F. Dowell are also gratefully acknowledged.

References and Notes

(1) Finkelmann, H.; Rehage, G. *Adv. Polym. Sci.* **1984**, *60–61*, 99.
(2) Meurisse, P.; Noel, C.; Monnerie, L.; Fayolle, B. *Br. Polym. J.* **1981**, *13*, 55.
(3) Krigbaum, W. R.; Watanabe, J. *Polymer* **1983**, *24*, 1299.
(4) Watanabe, J.; Hayashi, M. *Macromolecules* **1988**, *21*, 278; **1989**, *22*, 4083.
(5) Bello, A.; Pérez, E.; Marugán, M. M.; Pereña, J. M. *Macromolecules* **1990**, *23*, 905.
(6) Pérez, E.; Bello, A.; Marugán, M. M.; Pereña, J. M. *Polym. Commun.* **1990**, *31*, 386.
(7) Pérez, E.; Riande, E.; Bello, A.; Benavente, R.; Pereña, J. M. *Macromolecules* **1992**, *25*, 605.
(8) Schaefer, J.; Stejskal, E. O.; Buchdahl, R. *Macromolecules* **1977**, *10*, 384.
(9) VanderHart, D. L.; Earl, W. L.; Garroway, A. N. *J. Magn. Reson.* **1981**, *44*, 361.
(10) Möller, M. *Adv. Polym. Sci.* **1985**, *66*, 59.
(11) Horii, F.; Hirai, A.; Kitamuru, R. *Polym. Bull.* **1983**, *10*, 357.
(12) Earl, W. L.; VanderHart, D. L. *Macromolecules* **1979**, *12*, 762.
(13) Abragam, A. *The Principles of Nuclear Magnetism*; Oxford University Press: Oxford, U.K., **1961**.
(14) Connor, T. M. *Nucl. Magn. Reson.* **1971**, *4*, 247.
(15) VanderHart, D. L.; Atalla, R. H. *ACS Symp. Ser.* **1987**, *340*, 88.
(16) Fyfe, C. A. *Solid State NMR for Chemists*; CFC Press: Guelph, Ontario, Canada, **1983**; Chapter 7.
(17) González, C. C.; Bello, A.; Pereña, J. M. *Makromol. Chem.* **1989**, *190*, 1217.
(18) Bello, A.; Riande, E.; Pérez, E.; Marugán, M. M.; Pereña, J. M. *Macromolecules* **1993**, *26*, 1072.
(19) Certain commercial companies are named in order to specify adequately the experimental procedure. This in no way implies endorsement or recommendation by the authors or their agencies.
(20) Torchia, D. A. *J. Magn. Reson.* **1978**, *30*, 613.
(21) Vega, A. J.; Vaughan, R. W. *J. Chem. Phys.* **1978**, *68*, 1958.
(22) Rhim, W.-K.; Elleman, D. D.; Vaughan, R. W. *J. Chem. Phys.* **1973**, *59*, 3740.
(23) Pereña, J. M.; Marugán, M. M.; Bello, A.; Pérez, E. *J. Non-Cryst. Solids* **1991**, *131*, 893.
(24) Brown, G. H.; Doane, J. W.; Neff, V. D. *A Review of the Structure and Physical Properties of Liquid Crystals*; CRC Press: Cleveland, OH, **1971**; pp 45–46.
(25) VanderHart, D. L. *J. Chem. Phys.* **1986**, *84*, 1196.
(26) Tonelli, A. E. *Macromolecules* **1978**, *30*, 565.
(27) Pople, J. A. *J. Chem. Phys.* **1956**, *24*, 1111.
(28) VanderHart, D. L. *J. Magn. Reson.* **1987**, *72*, 13.
(29) Garroway, A. N.; Moniz, W. B.; Resing, H. A. *ACS Symp. Ser.* **1979**, *103*, 67.
(30) Maricq, M. M.; Waugh, J. S. *J. Chem. Phys.* **1979**, *70*, 3300.
(31) Strobl, G. R.; Schneider, M. *J. Polym. Sci., Polym. Phys. Ed.* **1980**, *18*, 1343.
(32) Kent, S.; Brennen, J. E.; Geil, P. H. *J. Mater. Sci. Lett.* **1991**, *10*, 1456.
(33) Takahashi, T., Nagata, F. *J. Macromol. Sci., Phys.* **1989**, *B28*, 349.